

compared with those reported for the purely siliceous ITQ-7<sup>[5]</sup>. This can probably be attributed to the presence of Ge in the framework. An interesting observation is that while the purely siliceous sample presents crystallite sizes of  $\sim 2.0 \mu\text{m}$ , Ge-ITQ-7 forms very small crystallites with dimensions ( $> 0.1 \mu\text{m}$ ) close to those of nanocrystalline zeolites (Figure 7). This result is extremely interesting, from the catalytic point of view, when treating molecules with smaller diffusion coefficients.

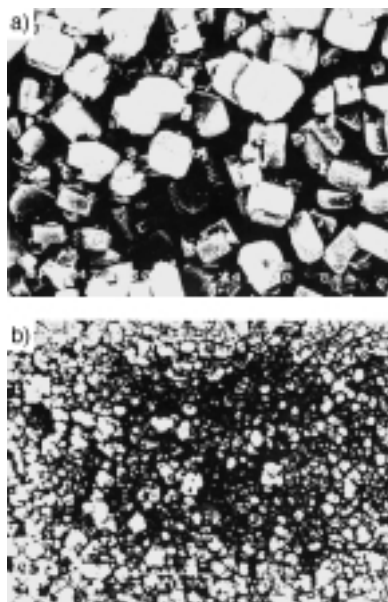


Figure 7. Scanning electron micrographs of a) purely siliceous ITQ-7 and b) Ge-ITQ-7.

After succeeding in the synthesis of Ge-ITQ-7, the incorporation of Al was attempted by preparing a gel with of composition  $\text{SiO}_2:\text{GeO}_2:\text{Al}_2\text{O}_3:\text{C}_{14}\text{H}_{26}\text{NOH}:\text{HF}:\text{H}_2\text{O}$  in a molar ratio 1.0:0.10:0.02:0.55:0.55:3.30. After 7 days crystallization at 423 K, Al/Ge-ITQ-7 was obtained (Figure 1c). The Al content was 1.2 wt % in the form of  $\text{Al}_2\text{O}_3$ . The  $^{27}\text{Al}$  MAS NMR spectrum (Figure 3b) indicates that the majority of Al is tetrahedrally coordinated ( $\delta = 54$ ) but some octahedral Al ( $\delta = 0$ ) is present. In the IR spectrum of Al/Ge-ITQ-7 after pyridine adsorption (spectrum not shown), a  $\tilde{\nu} = 1545 \text{ cm}^{-1}$  band attributed to pyridinium ions is observed, which indicates that this sample possesses a strong acidity.

The catalytic behaviour of the Al/Ge-ITQ-7 was tested by means of the catalytic cracking of *n*-decane and the results (Figure 5) indicate that the activity of this sample is lower than the B/Al-ITQ-7. This is in agreement with the greater amount of extra-framework Al present in Al/Ge-ITQ-7.

In conclusion, the  $\text{T}^{\text{III}}$ - and  $\text{T}^{\text{IV}}$ -substituted ITQ-7 zeolites have been synthesized and acid catalysts could be derived. For B-ITQ-7, boron occupies framework positions and generates mildly acid sites. The B can be exchanged with Al and, in the resultant B/Al-ITQ-7, the Al is in mostly in tetrahedral framework positions, to generate strongly acid sites that are very active for the cracking of *n*-decane. Germanium can also be introduced in the framework by direct synthesis, with a

concomitant modification in the morphology of ITQ-7. When Ge is present in the synthesis gel, Al can be directly introduced in the framework of ITQ-7. The resultant Al/Ge-ITQ-7 zeolite is also acidic and catalytically active.

Received: February 21, 2000 [Z14749]

- [1] A. Corma, *Chem. Rev.* **1995**, 95, 559.
- [2] H. Hamdan, B. Sulikowski, J. Klinowski, *J. Phys. Chem.* **1989**, 93, 350.
- [3] S. W. Kaiser, US Patent 4499327, **1985**; [*Chem. Abstr.* **1984**, 101, 24133v]; C. D. Chang, *Catal. Rev. Sci. Eng.* **1984**, 26, 323.
- [4] Y. Kubota, M. M. Helmkamp, S. I. Zones, M. E. Davis, *Microporous Mater.* **1996**, 6, 213.
- [5] L. A. Villaescusa, P. A. Barret, M. A. Cambor, *Angew. Chem.* **1999**, 111, 2164; *Angew. Chem. Int. Ed.* **1999**, 38, 1997.
- [6] L. A. Villaescusa, PhD thesis, Universidad Polit cnica de Valencia (Spain), **1999**.
- [7] R. Bandyopadhyay, Y. Kubota, N. Sugimoto, Y. Fukushima, Y. Sugi, *Microporous Mesop. Mater.* **1999**, 32, 81.
- [8] L. J. Bellamy, *The Infrared Spectra of Complex Molecules*, Chapman and Hall, London, **1975**.
- [9] R. F. Lobo, M. E. Davis, *Microporous Mater.* **1994**, 3, 61.
- [10] T. Takewaki, L. W. Beck, M. E. Davis, *Microporous Mesop. Mater.* **1999**, 33, 197.
- [11] C. M. Zicovich-Wilson, A. Corma, *J. Phys. Chem. B* **2000**, 104, 4134.

## Infinite, Linear, Unbranched Borynide Chains in $\text{LiB}_x$ —Isoelectronic to Polyene and Polycumulene\*\*

Michael W rle\* and Reinhard Nesper\*

*Dedicated to Professor Peter Paetzold  
on the occasion of his 65th birthday*

One of the great challenges in carbon chemistry is the synthesis of unbranched, linear chain modifications of carbon, the carbynes. Such carbynes are expected to have interesting physical properties like exceptional mechanical strength as well as one-dimensional conductivity and display an unusual variety of soliton and polaron states under appropriate doping conditions.<sup>[1]</sup> An infinite, linear, unbranched carbon chain can adopt the acetylenic  $-\text{[C}\equiv\text{C]}_n\text{C}\equiv$  ( $\alpha$  carbyne) or the cumulenic form  $=\text{[C=]}_n\text{C=}$  ( $\beta$  carbyne).<sup>[1–3]</sup> A main problem in synthesizing these carbon chains is their tendency to undergo interchain polymerization reactions of the Diels–Alder type.<sup>[2, 4, 5]</sup>

[\*] Dr. M. W rle, Prof. Dr. R. Nesper  
Laboratory of Inorganic Chemistry  
ETH Z rich  
Universit tsstrasse 6, 8092 Z rich (Switzerland)  
Fax: (+41) 1-632-1149  
E-mail: nesper@inorg.chem.ethz.ch

[\*\*] The financial support by the Swiss National Science Foundation (projects 21-36586.92 and 4030-032775) is gratefully acknowledged. We thank Dr. V. Shklover for SEM pictures, Dr. M. Spahr for magnetic measurements, Dr. T. Chatterij and Dr. E. Souard for the neutron diffraction experiments, and Prof. Dr. S. Roth, Prof. Dr. H. Kuzmany, Prof. H. D. Lutz, and Dr. E. Suchanek for spectroscopic investigations.

One way to keep short chains separated from each other is to introduce specific end groups. For chains with up to 16  $C_2$  units, a stabilization seems to be possible in that way.<sup>[6–8]</sup> Not long ago, Bauer et al. reported the formation of small boron carbon chains containing up to 13 atoms in a rare earth metal matrix.<sup>[9, 10]</sup>

We have now extended this idea to a polar, charged, pseudoelement system, namely, a lithium boride in which each boron atom yields one negative charge and thus becomes isoelectronic to carbon. The compound forms from a low-temperature melt of lithium and boron showing increasing viscosity with temperature and time,<sup>[11–13]</sup> which is traced back to the presence of different oligo and polymeric boron species in the melt before solidification either to an apparently metallic glass or the crystalline  $LiB_x$  depending on the actual composition and tempering time. If about 10% magnesium is added to the lithium melt, the metallic glass behavior is more pronounced.<sup>[14]</sup> Over more than twenty years, different groups<sup>[15, 16]</sup> have tried to unravel the nature of the polymerization products and of the compound  $LiB_x$ . Lithium-rich boron alloys possibly doped by a few percent of magnesium have been proposed as lithium electrode materials.<sup>[17, 18]</sup> We now succeeded in preparing pure-phase  $LiB_x$  samples with the approximate range  $0.82 < x < 1.0$ . The upper limit is somewhat unclear, since detection of an excess of poorly crystalline boron in the powder diagrams is very difficult. Furthermore, we were able to solve the crystal structure, which revealed a novel linear borynide chain that can be described as the first linear boron wire of molecular dimension. The borynide chain  $[B^-]_n$  is indeed an exciting example of how some longstanding problems in materials science, in this case the synthesis of carbyne  $C_n$ , may be circumvented by a pseudoatom approach ( $B^-$  instead of  $C$ ).<sup>[19]</sup>

We report here on the preparation and structural characterization of  $LiB_x$ , which contains linear, unbranched borynide chains in a lithium matrix. A compound with the same powder patterns was described earlier as either  $Li_5B_4$  ( $x=0.80$ ) or  $Li_7B_6$  ( $x=0.85$ ).<sup>[15, 21]</sup> In these investigations a structure containing three rings of boron atoms with unreasonably short distances was proposed based on an erroneous pseudo-cubic, rhombohedral symmetry. Study of the powder patterns showed that there are additional strong Bragg reflections which were misinterpreted in these older investigations. Proper indexing of the pattern led us to a hexagonal metric which depends on the stoichiometry parameter  $x$ .<sup>[16]</sup>

Our investigation is based on pure-phase  $LiB_x$  obtained as a brittle, grey, metallic solid upon heating elemental lithium and  $\beta$ -rhombohedral boron in sealed steel or niobium ampoules under an argon atmosphere for 48 h at 723 K. Scanning electron microscopy pictures show that this solid is composed of thin fiberlike crystals (Figure 1).<sup>[22]</sup> The compound is very sensitive to oxygen, nitrogen, and water and can be handled only under an inert argon atmosphere without decomposition. Finely ground powders are pyrophoric upon contact with air. As expected for such polymers, attempts to grow larger single crystals suitable for crystal structure determination failed up to now. Therefore, we used X-ray and neutron powder diffraction data for solving the structure. A close inspection of the X-ray powder diffraction patterns reveals that the

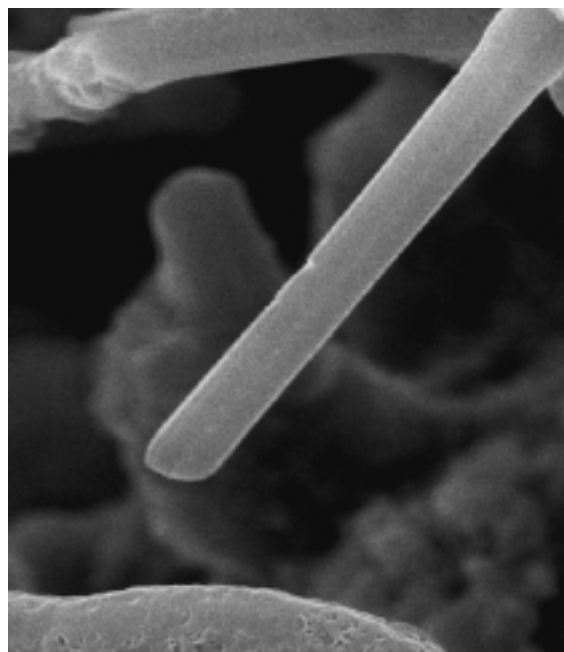


Figure 1. SEM picture of  $LiB_x$  crystals (length 36  $\mu m$ , diameter 4  $\mu m$ ). In the upper left corner one can see partly decomposed fibers, due to exposure to air.

positions of some lines vary with the lithium content of the sample, whereas other lines remain unaffected. Instead of assuming two different phases in the samples (as proposed by Wang et al.),<sup>[11, 12]</sup> we were able to index all the observed lines consistently on the basis of a single hexagonal unit cell. Depending on the lithium content, the lattice constants vary significantly. For nominal compositions  $x = 1.0$  and  $x = 0.82$  we find  $a = 4.025(1) \text{ \AA}$ ,  $c = 2.857(2) \text{ \AA}$ ,  $V = 40.08 \text{ \AA}^3$  and  $a = 4.019(1) \text{ \AA}$ ,  $c = 2.792(1) \text{ \AA}$ ,  $V = 39.06 \text{ \AA}^3$ , respectively. This is a volume reduction of nearly 3%, which is mainly due to the reduction of the  $c$  axis while the variations in the hexagonal base are unspecific. A structure model (Figure 2a) was worked out in space group  $P6_3/mmc$  and refined by simultaneous Rietveld refinement of multiple data sets (Figure 3) with X-ray and neutron powder diffraction data from samples of the nominal composition  $LiB_{0.82}$ .<sup>[23]</sup>

The structure may be derived from a hexagonal closed packing of Li atoms, but the  $c/a$  ratio (0.7098, 0.6947) is so

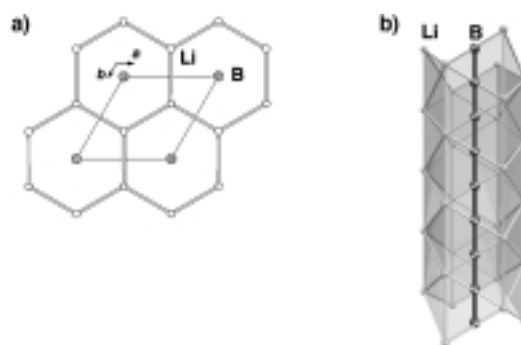


Figure 2. a) The unit cell of  $LiB_x$  in the [001] projection; b) a chain of boron atoms surrounded by a lithium shell. One possible location of the B atoms in the disordered borynide chain is shown.

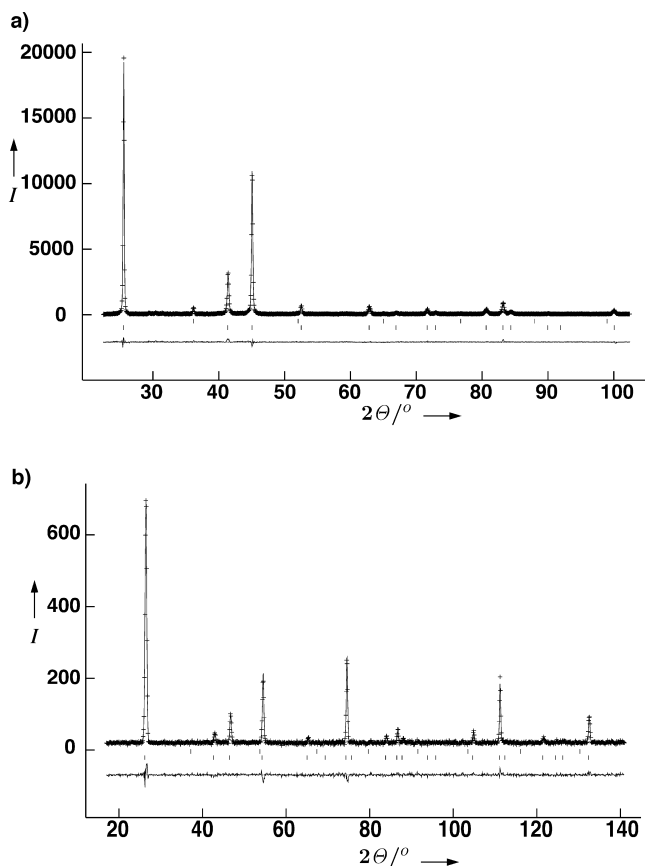


Figure 3. Multiple data set Rietveld refinement (after background correction) with a) X-ray and b) neutron powder diffraction data on samples with the nominal composition  $\text{LiB}_{0.82}$ .

different from the ideal one (1.633) that this correlation would be too far fetched. The original stacks of face-sharing  $\text{Li}_6$  octahedra along the  $c$  direction fuse to a sixfold column which fully encapsulates the boron strand (Figure 2b). The boron positions cannot be defined with atomic resolution in the direction of the chain, as shown by the characteristic electron density section displayed in Figure 4. This is due to the

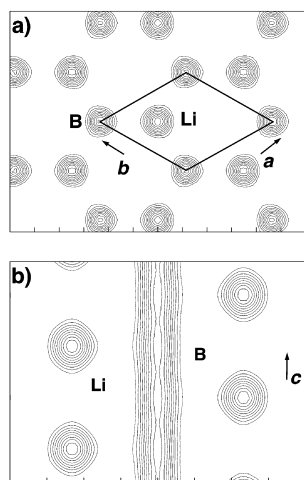


Figure 4. Observed electron density distribution in  $\text{LiB}_x$ : a) layer perpendicular to  $[001]$  at  $z = 0.25$ ; b) layer perpendicular to  $[110]$  through the origin of the unit cell to show the disordered boron atom sites (line distance of  $0.3 \text{ e}^- \text{Å}^{-3}$ ).

particular bonding requirements of lithium and boron in this compound (see below).

Similar electron density distributions are observed in composite structures where two partial structures form incommensurate arrangements. This may either give rise to satellite reflections or regions of expanded diffuse scattering depending on the degree of disorder. In the latter case, layers of diffuse intensity are expected perpendicular to the boron chain direction, and the lower edge of the diffuse intensity is a measure of the average boron–boron distance. Such behavior is observed, for example, in apatites with incommensurate distribution of the anions in the channels.<sup>[25]</sup> Indeed, very weak diffuse intensity is detected in the X-ray patterns, and strong diffuse scattering appears in the neutron diffraction pattern. In both cases this onset occurs at  $d = 1.59 \text{ Å}$ , which we interpret as the average B–B distance in the chains (Figure 5).

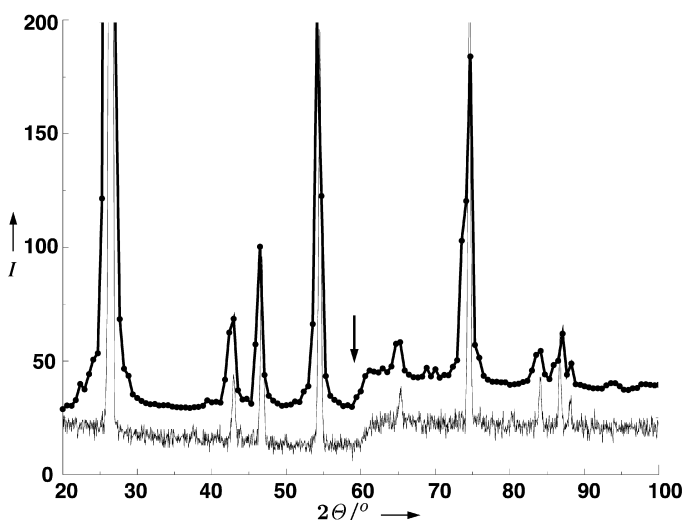


Figure 5. Selected area of the neutron diffraction pattern (lower curve) with the step-like diffuse scattering and simulated pattern (upper curve).

This is significantly longer than the simplest commensurate model with  $d(\text{B} - \text{B}) = c/2 = 1.396 \text{ Å}$  and thus two bonds per unit cell, the latter being too short with respect to the bonding situation of (approximately) four bonds for each boron atom as dictated by the valence electron count. Accordingly, the simulated<sup>[26]</sup> diffuse intensity step (Figure 5) is based on a model containing 400 boron chains ( $20 \times 20 \times 20$  superstructure, 32 000 atoms) with alternating single and triple bonds of  $1.40 \text{ Å}$  and  $1.77 \text{ Å}$  (av  $1.59 \text{ Å}$ ), respectively, which are randomly shifted against each other along the  $c$  axis. However, a related conjugated chain model with average spacing between the boron atoms leads to the same result. Thus the diffraction data do not allow discrimination between the two limiting cases. This smeared out appearance of the boron chains based on the diffraction data shows that there is practically no correlation between different chains, but instead disorder. The kink at  $d = 1.59 \text{ Å}$  is very well reproduced by this model, as shown in Figure 5.

Comparing the mean boron–boron distances derived from the kinks in the scattering data and the  $c$  lattice translation, the lithium-to-boron ratio is obtained. The former defines the

(fractional) number of borons and the latter the (integer) number of lithium atoms per unit cell. Compositions of  $\text{LiB}_{0.90}$  and  $\text{LiB}_{0.88}$  are calculated, whereas the above-mentioned hypothetical commensurate chain length would lead to stoichiometric  $\text{LiB}$ . The composition calculated by means of free occupancy and temperature factor refinement is  $\text{LiB}_{0.95(1)}$ . A composition of  $\text{LiB}_{0.88}$  can be refined to practically the same  $R$  value as in the free refinement, that is, the variation of  $R$  due to these model changes is insignificant (Table 1). The residual electron density is very weak and featureless (see Figure 4). No substantial number of defects in the boron chains are to be expected, because that would reduce the boron content even further below  $x = 0.88$ , resulting in a significant increase of the figure of merit.

Table 1. Atomic coordinates, isotropic thermal displacement parameters ( $U_{\text{iso/equi}}$ ), and site occupation factors (Occ.) obtained from free refinement of thermal parameters and site occupation factors.

Atom	Site	$x$	$y$	$z$	Model A <sup>[a]</sup>		Model B <sup>[b]</sup>	
					$U_{\text{iso/equi}}$ [Å]	Occ.	$U_{\text{iso/equi}}$ [Å]	Occ.
Li	2c	1/3	2/3	1/4	0.0305(6)	1	0.0398(5)	1
B1	2a	0	0	0	0.0295(6)	0.48(1)	0.0283(5)	0.44
B2	2b	0	0	1/4	0.0295(6)	0.47(1)	0.0283(5)	0.44

[a] Model A: free refinement leading to the composition  $\text{LiB}_{0.95(2)}$  ( $wRp = 0.159$ ). The estimated standard deviations of the occupation factors for model A have been multiplied by a factor of 3 with respect to the calculated results, accounting for the well-known oversampling effects in the Rietveld refinement. [b] Model B: for a constrained composition of  $\text{LiB}_{0.88}$  ( $wRp = 0.160$ ).

A small excess of lithium in the sample with the nominal composition  $\text{LiB}_{0.82}$  is detected in the X-ray powder diffraction pattern. This excess cannot easily be removed due to the sensitivity of  $\text{LiB}_x$  to loss of lithium under vacuum conditions.

An interesting question is how much charge the corresponding—still hypothetical—carbyne chain would take up from a surrounding Li matrix. By comparison with  $n$ -doped polyacetylene chains it is expected to do so.<sup>[27]</sup> The chains in  $\text{LiB}_x$  may also be slightly reduced by population of  $\pi^*$  states depending on the actual composition. Because of the phase width the bond order in the chains can show slight changes. On the other hand, a population of bonding lithium states is more likely and, as such, is reflected by the significant reduction of the  $c$  axis with increasing lithium content. These two effects induce a metal conductivity ( $\sigma = 7 \times 10^6 \text{ S cm}^{-1}$ ),<sup>[11]</sup> which is different from all other lithium borides known so far.<sup>[28, 29]</sup> The variable lithium content plays the same role here as oxidizing or reducing dopants, which are in general a necessary ingredient for achieving conducting, carbon-based polymers. Considering an ideal valence electron concentration (VEC) of four for the boron atoms, the same bonding situation as for a carbyne chain is present. This is matched by assigning formal charges of  $-1$  to all boron atoms. The bonding situation is expected to be very similar to that calculated for the hypothetical carbon chain, namely,  $=[\text{B}^-]_n\text{B} =$  or  $-\text{[B}^-\equiv\text{B}^-]_n\text{B}^-$ .

The description of an ionic compound is also in agreement with  $^7\text{Li}$  NMR measurements which reveal a series of lines

around  $\delta = 0$  with respect to an aqueous solution of lithium chloride<sup>[22]</sup> as well as with *ab initio* and extended Hückel calculations for small boron–carbon chains.<sup>[9]</sup> The chains of pseudocarbon atoms  $\text{B}^-$  in  $\text{LiB}_x$  are the first examples of carbinoid systems (borynide) of a really large size.

According to MP2 calculations, the distances for a  $\text{B}=\text{B}$  bond should lie in the range of  $1.629 \text{ Å}$  for the hypothetical molecule  $\text{Li}_2\text{B}_2\text{H}_4$ , where the  $\text{B}_2\text{H}_4^{2-}$  anion is coordinated by two  $\text{Li}^+$  cations, and  $1.673 \text{ Å}$  for the isolated ion.<sup>[30]</sup> These bond distances are only marginally shorter than the observed single bond distances in organic derivatives of  $\text{B}_2\text{H}_4$  ( $1.698(4)$ ,  $1.711(6) \text{ Å}$ ),  $\text{B}_2\text{F}_4$  ( $1.67(5)$ ,  $1.72 \text{ Å}$ ),  $\text{B}_2\text{Cl}_4$  ( $1.75(5)$ ,  $1.70(7) \text{ Å}$ ), and  $\text{B}_2\text{Br}_4$  ( $1.69(2) \text{ Å}$ ). A comparison of the boron–boron bond distances for different neutral, singly and doubly reduced organodiborane(4) compounds<sup>[31]</sup> reveals a shortening upon going from the neutral species ( $1.706(12)$  and  $1.724(9) \text{ Å}$ , bond order of one) to the doubly reduced species ( $1.627(9)$  and  $1.636(11) \text{ Å}$ , bond order two). Apparently, the shortening due to higher bond order is reduced by the increasing coulombic repulsion. In any case, the average boron–boron distance of  $1.59 \text{ Å}$  in  $\text{LiB}_x$  is at the short end of the expected values for  $\text{B}=\text{B}$  bonds. A significant shortening of single bond distances is also observed in conjugated carbon chain systems.<sup>[32]</sup> Furthermore, the coulombic attraction of the lithium matrix, the length of a  $\text{B}=\text{B}$  bond, and the coulombic repulsion within the boron chains are competing effects and difficult to weigh against each other. The Li–B distances are comparable with those in other lithium borides ( $2.321(1) - 2.424(1) \text{ Å}$ ).<sup>[29, 33]</sup> The lithium atoms form a continuous one-dimensional cage which encapsulates and stabilizes the boron chain like an insulation shell around a wire.

Solid-state NMR experiments<sup>[22]</sup> support a description such as  $(\text{Li}^+)_x(\text{B}^-)$  where the lithium atoms have mainly cationic character. However, a small amount of electron density centered at Li is quite likely, especially because the Li matrix contracts with increasing electron number. This will lead to metallic conductivity as well. The unique structure of this compound leads to very interesting physical and spectroscopic properties.<sup>[1]</sup> The binary phase system lithium–boron was investigated by several authors. A lithium boride in the mentioned composition range was used as an electrode material due to its unique properties: The material releases and takes up elemental lithium due to its high microporosity, and it exhibits a high mechanical stability even at temperatures above the melting point of lithium.<sup>[21, 22]</sup> Sanchez and Belin showed that samples of nominal composition  $\text{Li}_7\text{B}_3$  consist of a refractory matrix of the composition  $\text{LiB}_{0.943}$  and elemental lithium.<sup>[22]</sup> This observation can be explained by our results as well as the shape of the crystals formed and the difficulties encountered in growing single crystals.

The high microporosity and the possibility of the inclusion of metal explains the very different values for the experimentally determined densities reported in the literature.<sup>[12, 22, 34, 35]</sup> Conductivity measurements<sup>[11, 16]</sup> on the system described here show metallic behavior, in contrast to all other known binary lithium borides. This can be explained by the special charge transfer situation between the boron chains and the lithium matrix. At present, corresponding theoretical investigations are being performed. Magnetic measurements

show a hysteresis of the magnetization curve at 5 K, the nature of which is not understood but which may be due to a Peierls distortion in the borynide chains. This correlates nicely with the observation of additional Bragg reflections in the neutron diffraction pattern at low temperature. To our knowledge, the borynide chain  $[B^-]_n$  in  $LiB_x$  is the first structurally well characterized linear system which is isoelectronic and isolobal to carbyne.

Received: September 17, 1999

Revised: March 21, 2000 [Z 14027]

- [1] M. J. Rice, A. R. Bishop, D. K. Campbell, *Phys. Rev. Lett.* **1983**, *51*, 2136.
- [2] R. Hoffmann, C. Janiak, C. Kollmar, *Macromolecules* **1991**, *24*, 3725.
- [3] F. Cataldo, *Polym. Int.* **1997**, *44*, 191.
- [4] F. Diederich, *Nature* **1994**, *369*, 199.
- [5] F. Diederich, Y. Rubin, *Angew. Chem.* **1992**, *104*, 1123; *Angew. Chem. Int. Ed. Engl.* **1992**, *31*, 1101.
- [6] T. Bartik, B. Bartik, M. Brady, R. Dembinsky, J. A. Gladysz, *Angew. Chem.* **1996**, *108*, 467; *Angew. Chem. Int. Ed. Engl.* **1996**, *35*, 414.
- [7] R. E. Martin, F. Diederich, *Angew. Chem.* **1999**, *111*, 1440; *Angew. Chem. Int. Ed.* **1999**, *38*, 1350.
- [8] J. Bauer, J.-F. Halet, J.-Y. Saillard, *Coord. Chem. Rev.* **1998**, *178–180*, 723.
- [9] J. Bauer, G. Boucekkine, G. Frapper, J.-F. Halet, J.-Y. Saillard, B. Zouchoune, *J. Solid State Chem.* **1997**, *133*, 190.
- [10] D. Ansel, J. Bauer, F. Bonhomme, G. Boucekkine, G. Frapper, P. Gougeon, J.-F. Halet, J.-Y. Saillard, B. Zouchoune, *Angew. Chem.* **1996**, *108*, 2245; *Angew. Chem. Int. Ed. Engl.* **1996**, *35*, 2098.
- [11] F. E. Wang, R. A. Sutula, M. A. Mitchell, J. R. Holden, *Naval Surface Weapons Center, TR 77–84*, **1977**.
- [12] F. E. Wang, M. A. Mitchell, R. A. Sutula, J. R. Holden, *J. Less-Common Met.* **1978**, *61*, 237.
- [13] M. Wörle, Diplom thesis, Universität Stuttgart, Max-Planck-Institut für Festkörperforschung, Stuttgart, **1990**.
- [14] W. B. Pearson, personal communication, **1984**.
- [15] F. E. Wang, *Metall. Trans. A* **1979**, *10*, 343.
- [16] M. Wörle, PhD thesis, ETH Zürich, no. 11162, **1995**.
- [17] R. A. Sutula, F. E. Wang (US Navy), US-A 4162352, **1979** [*Chem. Abstr.* **1979**, *91*, 126104j].
- [18] F. Riffault, C. Pathé, S. Ferrier, D. Debattista (Aerospatiale), EP-B 160604, **1985** [*Chem. Abstr.* **1986**, *104*, 53681v].
- [19] Recently, Daedalus envisaged a stabilization of carbyne chains by metal coordination.<sup>[20]</sup>
- [20] D. Jones, *Nature* **1995**, *327*, 636.
- [21] S. Dallek, D. W. Ernst, B. F. Larrick, *J. Electrochem. Soc.* **1979**, *126*, 866.
- [22] P. Sanchez, C. Belin, *C. R. Seances Acad. Sci. Ser. II* **1988**, *307*, 2021.
- [23] The simultaneous Rietveld refinement was performed with the Program package GSAS.<sup>[24]</sup> The X-ray data were obtained on a Stoe STADIP powder diffractometer, and the neutron powder diffraction data were recorded at the D2B beamline at the ILL in Grenoble. The following *R* values were obtained: neutron: *wRp* = 0.107, *Rp* = 0.082, *R(F<sup>2</sup>)* = 0.084 (28 observed reflections); X-ray: *wRp* = 0.164, *Rp* = 0.103, *R(F<sup>2</sup>)* = 0.096 (22 observed reflections); total: *wRp* = 0.160, *Rp* = 0.102 (see Table 1). Further details on the crystal structure investigation may be obtained from the Fachinformationszentrum Karlsruhe, 76344 Eggenstein-Leopoldshafen, Germany (fax: (+49) 7247-808-666; e-mail: crysdata@fiz-karlsruhe.de), on quoting the depository number CSD-410955.
- [24] A. C. Larson, R. B. Von Dreele, Program GSAS, Los Alamos, **1994**.
- [25] P. Alberius-Henning, PhD thesis, Stockholm University, **1999**.
- [26] T. Proffen, R. B. Neder, Program DISCUS, *J. Appl. Cryst.* **1997**, *30*, 171. A program to extract powder data from the calculated diffraction patterns was written by us.
- [27] S. Roth, *One-dimensional Metals*, VCH, Weinheim, **1995**.
- [28] G. Mair, PhD thesis, Universität Stuttgart, **1984**.

- [29] G. Mair, H. G. von Schnering, M. Wörle, R. Nesper, *Z. Anorg. Allg. Chem.* **1999**, *625*, 1207.
- [30] E. Kaufmann, P. von R. Schleyer, *Inorg. Chem.* **1988**, *27*, 3987.
- [31] W. J. Grigsby, P. Power, *Chem. Eur. J.* **1997**, *3*, 368.
- [32] G. Gilli in *Fundamentals of Crystallography* (Ed.: C. Giacovazzo), Oxford University Press, Oxford, **1988**, p. 504.
- [33] G. Mair, R. Nesper, H. G. von Schnering, *J. Solid State Chem.* **1988**, *75*, 30.
- [34] M. A. Mitchell, R. A. Sutula, *J. Less-Common Met.* **1978**, *57*, 161.
- [35] V. P. Sorokin, P. I. Gavrilov, E. V. Levakov, *Russ. J. Inorg. Chem.* **1977**, *22*, 329.

## A New, Simple Route to Novel Gold Clusters: Structure of an $Au_6Ag$ Wheel with a Gold Rim\*\*

Elena Cerrada, María Contel, A. Delia Valencia, Mariano Laguna,\* Thomas Gelbrich, and Michael B. Hursthouse

Gold–silver clusters in which the gold and silver atoms can be formally considered in an oxidation state between 0 and 1,<sup>[1–7]</sup> have attracted considerable attention during the last decade. Apart from such clusters, few complexes containing unsupported gold–silver bonds, namely  $[AuAg(C_6F_5)_2L_2]_n$ ,<sup>[8, 9]</sup>  $[Au_2Ag_2(CH_2PPh_3)_4(CIO_4)_4]$ ,<sup>[10]</sup>  $[Au_3(\mu-bzim-N^3, C^2)_3]_2Ag$ ,<sup>[11]</sup> and  $[Au_4Ag(CH_2SiMe_3)_4(\mu-dppm)_2]CF_3SO_3$ <sup>[12]</sup> have been reported so far (L = tetrahydrothiophene, benzene; bzim = 1-benzylimidazole). For the latter two, the silver center is coordinated solely by gold atoms in a distorted trigonal prismatic and a distorted tetrahedral fashion, respectively.

In this communication, we report on the synthesis of novel heteronuclear compounds containing  $Au_5Ag$  and  $Au_6Ag$  cores. The X-ray crystal structure of the complex  $[Au_6Ag-\{\mu-C_6H_2(CHMe)_3\}_6]CF_3SO_3$  confirms the presence of an almost planar  $AgAu_6$  core, in which the silver(I) atom is at the center of a regular hexagon of gold atoms. Thus, a “cart wheel”-like arrangement is achieved, in which the six gold–gold interactions form the rim and the six silver–gold bonds the spokes. To the best of our knowledge, this coordination mode for a silver center does not have a precedent in the literature.

Heteronuclear gold–silver compounds (with unsupported metal–metal bonds) can be obtained by the addition of silver ions to dinuclear<sup>[12]</sup> or cyclic trinuclear gold(I) complexes.<sup>[11]</sup>

[\*] Prof. M. Laguna, Dr. E. Cerrada, Dr. M. Contel, A. D. Valencia  
Departamento de Química Inorgánica  
Instituto de Ciencia de Materiales de Aragón  
Universidad de Zaragoza-C.S.I.C., 50009 Zaragoza (Spain)  
Fax: (+34) 976-761187  
E-mail: mlaguna@posta.unizar.es  
Dr. T. Gelbrich, Prof. M. B. Hursthouse  
Department of Chemistry  
University of Southampton  
Highfield, Southampton, SO17 1BJ (UK)

[\*\*] This research was supported by the Dirección General de Enseñanza Superior (PB 98-0542) and the Engineering and Physical Sciences Research Council.